The effect of molecular architecture on the grain growth kinetics of A_nB_n star block copolymers

Xiaochuan Hu,[a] Yuqing Zhu,†[a] Samuel P. Gido,*[a] Thomas P. Russell,*[a] Hermis Iatrou,[b] Nikos Hadjichristidis,[b] Ferass M. Abuzaina[c] and Bruce A. Garetz[c]

[a] *Polymer Science and Engineering Department, University of Massachusetts, Amherst, Massachusetts, 01003, USA*
[b] *Department of Chemistry, University of Athens, Panepistimiopolis Zografou, 15771, Athens, Greece*
[c] *Department of Chemical and Biological Sciences and Engineering, Polytechnic University, Brooklyn, New York, 11201, USA*

Received 12th March 2004, Accepted 14th May 2004
First published as an Advance Article on the web 30th September 2004

To investigate the effect of molecular architecture on the grain growth kinetics of star block copolymers, a series of A_nB_n miktoarm star block copolymers with different numbers of arms (n = 1, 2, 4 and 16) was studied. Across this entire series of materials, all the A arms are polystyrene (PS) blocks from the same anionically synthesized batch, and thus all the A arms are identical. Likewise, all the B arms are polyisoprene (PI) blocks from the same anionically synthesized batch, and thus all the B arms are identical. All the stars employed in this study are therefore composed of the same A and B arms liked together in symmetric numbers. The coarsening kinetics of grain growth was monitored in real space by transmission electron microscopy (TEM), followed by subsequent micrograph image analysis. It was found that the molecular architecture influenced the grain growth kinetics of these A_nB_n star copolymers dramatically. The grain coarsening kinetics was found to follow a scaling law as $V \sim t^{\beta}$, where V is the characteristic grain volume and t is time. The exponent, β, was found to be about 0.2 for the diblock copolymer (n = 1) and 0.4 for all three of the star block copolymers (n = 2, 4 and 16) in the series. It is postulated that the difference in grain growth rate between the diblock and the various stars is due to a reduction in molecular entanglements resulting from chain stretching near the junction points in the stars.

Introduction

Block copolymers can microphase separate into ordered structures composed of lamellae, cylinders, and spheres, as well as a variety of other structures at temperatures below the order-to-disorder transition temperature.[1] When these materials are quiescently quenched from the disordered state to the ordered state, coherently ordered regions or grains form, often with different orientations. Grain size and structure have been shown to play an important role in determining the mechanical and

† Present address: Eastman Chemical Co., Kingsport, TN, USA.

transport properties of block copolymers.[2–5] Recent efforts to use block copolymers in microelectronic and photonic applications also requires precise control of the grain size and/or structure.[6,7]

Coherent grain orientation can be achieved by application of an external field, such as electric field,[8–13] surface,[14–16] shear,[17–19] temperature gradient,[20] *etc*. The kinetics of grain growth of diblock copolymers, both in the bulk and in thin films, has been investigated with a variety of techniques such as small angle X-ray scattering (SAXS),[21–23] transmission electron microscopy (TEM),[24,25] depolarized light scattering (DLS),[24,26–28] and atomic force microscopy (AFM).[29] In the microphase separated state, coherent order is interrupted by the presence of topological defects that can be zero- (point), one- (line), or two- (grain boundaries) dimensional. Also, since the block copolymers are relatively soft mesophase materials one also observes more continuous change in the local microstructural orientation akin to focal conic smectic liquid crystalline textures. Grain growth occurs by the motion and annihilation of these defects.[30] Many variables have been found that influence the ordering of block copolymers such as temperature (quench depth),[20,31] molecular weight, and molecular relaxation time.[32]

Prior research on block copolymer grain ordering kinetics has been focused on diblock copolymers. Little is known about the grain coarsening kinetics of star copolymers, especially the effect of molecular architecture on the coarsening kinetics. However, it has been well established that star copolymers behave differently from conventional diblock copolymers due to the molecular architecture effect in microphase separation,[33,34] domain spacing,[35–37] rheology and dynamics.[38–41] Meanwhile, advances in anionic living polymerization and arm coupling chemistries have made it possible to synthesize well-defined star copolymers.[42–44] Building upon these prior developments, the objective of the current work is to explore the effects of molecular architecture on the ordering kinetics of *miktoarm* star block copolymers. To achieve this end, a series of $(PS)_n(PI)_n$ miktoarm star copolymers ($n = 1$, 2, 4, and 16) are prepared using anionic living polymerization and chlorosilane coupling chemistry.[35] Most importantly, all the PS arms used in this series come from the same polymerization batch. So they are all characteristically the same. Likewise, all the PI arms are also the same. This enables us to exclude any variables from the study that would arise due to differences in the composition of constituting arms.

Experimental section

The A_nB_n star copolymers used in this study are prepared by living anionic polymerization of styrene and isoprene respectively, followed by controlled chlorosilane coupling chemistry and purification. Table 1 shows their molecular characteristics. Based on the composition of these A_nB_n stars, lamellar morphology is expected and confirmed experimentally for all these stars. The detailed synthesis, molecular and basic morphological characterization of these star copolymers has been published previously.[35]

Sample preparation

Five weight percent solutions of each of the four star copolymers were prepared in toluene, a neutral solvent for the PS and PI blocks. Bulk films about 1 mm thick were obtained by evaporating the

Table 1 Molecular characteristics of the PS_nPI_n star block copolymers

Sample	M_n[a]/g mol^{-1}	M_w[b]/g mol^{-1}	M_w/M_n[c]	PS (wt.%)[d]
PS arm	19 000	—	—	100
PI arm	15 000	—	—	0
PS_1PI_1	36 200	36 300	1.05	55 ± 2
PS_2PI_2	64 000	66 000	1.04	56 ± 2
PS_4PI_4	121 000	127 500	1.04	54 ± 2
$PS_{16}PI_{16}$	[e]	533 000	1.07	59 ± 2

[a] Membrane osmometry (MO) in toluene at 35 °C. [b] Low angle laser light scattering (LALLS) in THF at 25 °C. [c] Size exclusion chromatography in THF at 25 °C (DRI detector). [d] Measured by ^{1}H-NMR. [e] Too high to be measured by MO.

solvent from these solutions. Typically, studies of PS-PI block copolymer morphology involves covering the samples during solvent casting in order to slow solvent evaporation which takes place over one or two weeks.[35,45–48] In the present study, an initial microphase separated but not highly ordered state with small grains is desired. The size increase of these grains with thermal annealing will then be monitored. In order to produce an initial small grain size, the samples were cast without covering. The films thus produced were essentially solid after one day in air at room temperature, and were completely dry after two days. These dried films constituted the $t = 0$ initial point of the grain growth studies. Different pieces of these films were then annealed at 120 °C under vacuum for different periods of time to promote grain growth. To allow for quantitative comparison of grain size, all samples in this study are cast and annealed together to ensure that they experience identical external conditions. Different pieces of film for each of the samples were removed from the annealing oven at various times, from 30 min up to 60 days, and the grain size was characterized.

TEM characterization

All samples for transmission electron microscopy (TEM) were microtomed using a Leica Ultracut UCT cryoultramicrotome. Thin sections 50–100 nm in thickness are cut with a Diatome diamond knife at a temperature of −100 °C. In order to reduce sampling bias in the collection of TEM micrographs, several different sections of the sample were microtomed. These sections were then collected on 400 mesh copper TEM grids and stained in OsO_4 vapor for 6 hours. TEM was performed on either a JEOL 100CX or a JEOL 2000 FX instrument, operated at accelerating voltages of 100 kV or 200 kV respectively. TEM magnifications were calibrated with an etched silica size standard. Relatively low magnifications were used for all the micrographs to ensure that each micrograph encompasses as many entire grains as possible for the subsequent statistical analysis. A magnification of 8000× was used for samples during the early stages of grain growth, while a magnification of 6000× was used for the later stages of grain growth when the grains were larger. Forty to 50 TEM micrographs per sample per annealing time were used for the quantitative image analysis of grain size.

Quantitative image analysis

Grain size was obtained using the procedures described in detail by Garetz, Balsara and co-workers.[24,25,49] TEM micrographs were digitized and stored in TIFF files. Each digitized micrograph was divided into a total of 385×275 overlapping 32 pixel × 32 pixel squares with centers separated by 10 pixels, and the image within each square was stored as a 32×32 element array of 8-bit integers. The azimuthal angles, $\phi(\boldsymbol{r})$, which describe the local orientations of the lamellar normals at various points (given by the position vector $\boldsymbol{r}$) in the images relative to a fixed reference coordinate system, were computed by a local, two-dimensional Fourier transform (LFT). This LFT procedure produces a matrix of local azimuthal angles, $\phi(\boldsymbol{r})$, that describe the orientation of the projection of the lamellar normal in the image plane. This matrix is used to calculate the lamellar orientation correlation function, $C(\boldsymbol{r})$:[24]

$$C(|\boldsymbol{r}' - \boldsymbol{r}''|) = (15/8)\langle \sin^2\theta(\boldsymbol{r}')\sin^2\theta(\boldsymbol{r}'')\rangle\langle \cos\{2[\phi(\boldsymbol{r}') - \phi(\boldsymbol{r}'')]\}\rangle \approx \langle \cos\{2[\phi(\boldsymbol{r}') - \phi(\boldsymbol{r}'')]\}\rangle$$

The brackets $\langle \ldots \rangle$ represent an average over all pairs of points $\boldsymbol{r}'$ and $\boldsymbol{r}''$ in the ordered regions of a TEM micrograph. Since it is well established in the literature that lamellar microdomains are highly anisotropic in shape,[24,30,50,51] two different correlation functions, $C(\boldsymbol{r})_{\|}$ and $C(\boldsymbol{r})_{\perp}$, corresponding to the correlations in the direction of lamellar grain normal and perpendicular to this lamellar normal, have been evaluated. The parallel correlation function $C(\boldsymbol{r})_{\|}$ is calculated by averaging at points $\boldsymbol{r}'$ and $\boldsymbol{r}''$ where the vector $\boldsymbol{r}' - \boldsymbol{r}''$ is parallel to the lamellar grain normal within a prescribed tolerance of ±5°. Likewise, the perpendicular correlation function $C(\boldsymbol{r})_{\perp}$ is obtained by averaging at points $\boldsymbol{r}'$ and $\boldsymbol{r}''$ where the vector $\boldsymbol{r}' - \boldsymbol{r}''$ is perpendicular to the lamellar grain normal within a prescribed tolerance of ±5°. Both correlation functions were found to decay approximately exponentially. Thus, each correlation function curve was fit with an exponential form of $\exp(-r/\kappa)$, where κ is the correlation length. These correlation lengths are convenient parameters with which to characterize the grain size.

The procedure used in this study to obtain correlation lengths for TEM data was based on recently published methods[24] with the following exceptions: First, the correlation functions were obtained by systematically evaluating and summing the contributions from all pairs of 32×32 pixel boxes in each image. The analysis started with the first ordered box in the micrograph and

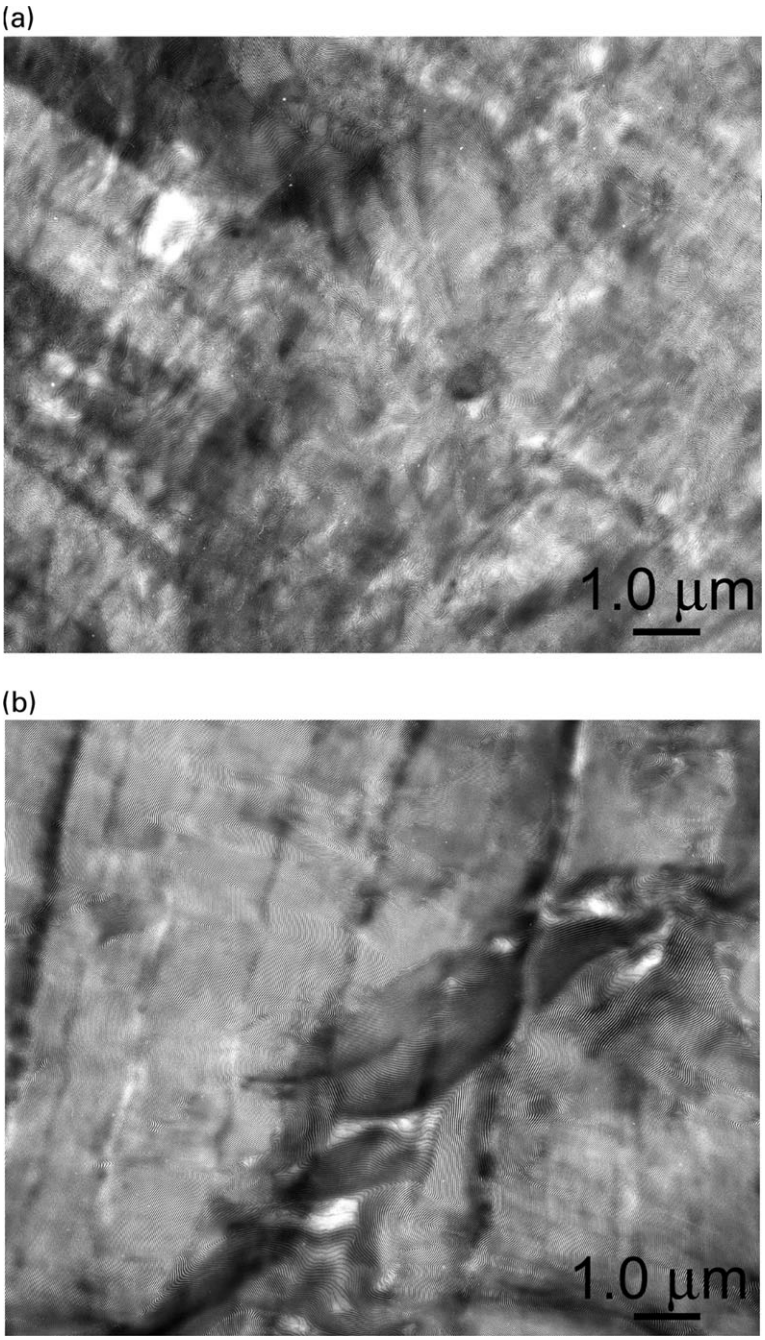

Fig. 1 Representative TEM images of PS_4PI_4 star block copolymer: (a) immediately after solution casting, *i.e.*, $t = 0$; and (b) after annealing for 60 days at 120 °C.

compared it with all the other ordered boxes in the same micrograph. Then the second box was compared to all other boxes, and so on until all the pairs of boxes in the micrograph have been compared. This contrasts with statistical sampling procedures used in a previously published study.[25] Also, since in this study the entire region in a micrograph is ordered with very few unclear regions and no disordered regions, the filtering process used in the previous studies[24] was not needed.

Results and discussion

Fig. 1a shows a TEM micrograph of the unannealed A_4B_4 sample, *i.e.* $t = 0$. Clearly the sample microphase separated in a lamellar morphology as a result of the solution casting, but the grain size is quite small. Fig. 1b shows a TEM image of the same A_4B_4 sample after annealing for 60 days, producing a significant increase in grain size.

As shown in Fig. 2a for the A_4B_4 material, both correlation functions, $C(r)_{\|}$ and $C(r)_{\perp}$, were found to approximately conform to the form of an exponential decay. Each curve is fit to an exponential function of the form $\exp(-r/\kappa)$, as shown in Fig. 2b, where κ is the correlation length, a characteristic dimension of the grain structure. The grains are generally anisotropic in shape, being larger parallel to the lamellar normal and smaller perpendicular to the lamellar normal. This has been reported previously in the literature for diblock copolymers[24,30,50,51] and is evident in our TEM of A_nB_n grain structure. Therefore, two characteristic correlation lengths are used to characterize each individual grain. The correlation length in the direction of lamellar normal is denoted as $\kappa_{\|}$, and the correlation length perpendicular to the lamellar normal is denoted as $\kappa_{\perp}$.

Both Table 2 and Fig. 3 show the time evolution of the characteristic grain size for the A_nB_n series of materials when annealed at 120 °C. The anisotropic grain shape is reflected in the fact that the $\kappa_{\|}$ values are consistently larger than the $\kappa_{\perp}$ values for all star functionalities and across the full range of annealing times, except for $A_{16}B_{16}$ at longer annealing times where $\kappa_{\|} \approx \kappa_{\perp}$. Least squares fits of power law functions of the form $\kappa = At^{\nu}$ are shown as lines on the graphs in Fig. 3. The A and ν parameters determined by these fits are given in Table 3. To within the error of the data, the $\kappa_{\|}$ and $\kappa_{\perp}$ fits, on the log-log scale in Fig. 3, are roughly parallel for each material. This indicates that the grain anisotropy does not change significantly during grain structure coarsening. The grain anisotropy for each sample can be approximated by the ratio of the constant, pre-exponential coefficients for the parallel and perpendicular correction lengths: $A_{\|}/A_{\perp}$. These values are 1.26, 1.52, 1.19, and 1.18 for A_1B_1, A_2B_2, A_4B_4, and $A_{16}B_{16}$, respectively. All of these grain anisotropy values are considerably lower than the previously reported value[50] of 2.37 for pre-impingement grain growth of lamellar forming diblock copolymers. The fact that the current studies focus on later stage grain size coarsening, after the initial growth and impingement process is complete, may unlie this discrepancy. A drive to reduce the overall amount of grain boundary surface area in the samples during grain coarsening will lead to lower grain anisotropy since surface to volume ratio is minimized for more compact, isotropic grain shapes.

In Fig. 4a all the parallel correlation lengths ($\kappa_{\|}$) for the A_nB_n series are plotted *vs.* time, and in Fig. 4b all the perpendicular correlation lengths ($\kappa_{\perp}$) are plotted *vs.* time. When the data is

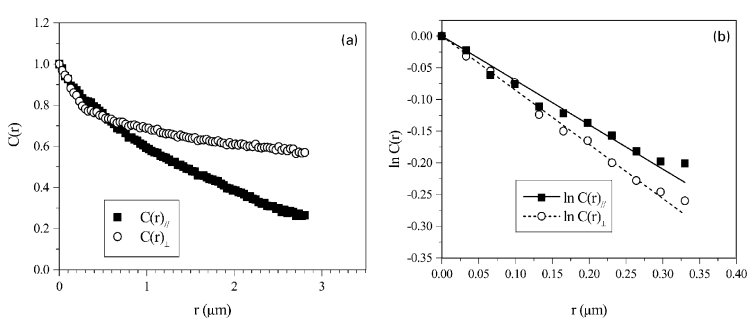

Fig. 2 Correlation functions for PS_4PI_4 parallel ($C_{\|}$) and perpendicular ($C_{\perp}$) to the lamellar normal after annealing at 120 °C for 60 days. (a) linear scale, and (b) logarithmic scale with least-squares exponential fit of the first 10 points of each correlation function.

Table 2 Correlation lengths determined by TEM image analysis. $\kappa_{\|}$ and $\kappa_{\perp}$ are correlation lengths parallel and perpendicular to the lamellar normal. $\sigma_{\|}$ and $\sigma_{\perp}$ are the standard deviations of $\kappa_{\|}$ and $\kappa_{\perp}$ respectively

	PS_1PI_1				PS_2PI_2			
Time/h	$\kappa_{\|}$/μm	$\sigma_{\|}$/μm	$\kappa_{\perp}$/μm	$\sigma_{\perp}$/μm	$\kappa_{\|}$/μm	$\sigma_{\|}$/μm	$\kappa_{\perp}$/μm	$\sigma_{\perp}$/μm
0	0.36	0.06	0.23	0.03	0.65	0.13	0.46	0.07
0.5	0.44	0.02	0.40	0.03	0.86	0.15	0.60	0.09
2	0.89	0.19	0.68	0.14	1.02	0.18	0.71	0.09
6	1.02	0.16	0.78	0.13	1.23	0.11	0.83	0.12
24	1.11	0.13	0.87	0.13	1.66	0.25	1.07	0.15
96	1.09	0.05	0.89	0.04	1.69	0.14	1.10	0.06
384	1.42	0.08	1.01	0.12	1.78	0.20	1.54	0.17
1440	1.45	0.16	1.04	0.04	1.97	0.14	1.71	0.07
	PS_4PI_4				$PS_{16}PI_{16}$			
0	0.42	0.04	0.43	0.04	0.37	0.03	0.32	0.03
0.5	0.47	0.10	0.45	0.11	0.45	0.03	0.33	0.03
2	0.68	0.10	0.55	0.07	0.43	0.03	0.38	0.03
6	0.82	0.15	0.55	0.09	0.49	0.05	0.48	0.04
24	0.99	0.12	0.84	0.16	0.62	0.07	0.61	0.07
96	1.02	0.03	0.87	0.04	0.63	0.05	0.62	0.05
384	1.39	0.04	1.15	0.08	0.85	0.09	0.84	0.11
1440	1.44	0.07	1.18	0.04	0.87	0.04	0.87	0.02

presented in this way, the relative grain size for different star functionalities can be seen. Fig. 5 shows plots of grain volume, estimated as $\kappa_{\|}\kappa_{\perp}\kappa_{\perp}$ *vs.* time for all the samples. Based on previous work by Balsara and co-workers[30] it is expected that the time evolution of average grain volume (V) obeys a power law: $V \sim t^{\beta}$. They reported that β for both pre- and post-impingement grain growth in a cylinder forming diblock copolymer of low molecular weight. The post-impingement β value of 1.20 is more relevant for comparison to our current results. Harrison *et al.*[29] has investigated the ordering kinetics in cylindrical diblock copolymer thin films and found that the correlation length increased with annealing time as $\sim t^{1/4}$.

The data in both Figs. 4 and 5 indicate that at any give time during the grain growth process the order of grain size among the samples from largest to smallest is generally A_2B_2, A_1B_1, A_4B_4, $A_{16}B_{16}$, except for the very longest times for which the order is: A_2B_2, A_4B_4, A_1B_1, $A_{16}B_{16}$. The volume *vs.* time plots are fit with power law functions of the form $V = At^{\beta}$, and the A and β parameters of this fit are given in Table 4. It is clear that the power law exponents (slopes in Fig. 5) for all the star architectures (A_2B_2, A_4B_4, and $A_{16}B_{16}$) are similar, in the range of 0.35 to 0.39. However, the power law exponent for the diblock, (A_1B_1), is very different, about 0.20. The grains of materials with star architectures are all growing at about the same rate and they are all growing faster than the grains of the diblock material. The grains of the diblock are bigger than those of the A_4B_4 and $A_{16}B_{16}$ stars, but the A_4B_4 grain size passes that of the diblock at long times. If the experiment could be extended to even longer times then the data suggests the $A_{16}B_{16}$ grain size

Table 3 Power law fitting parameters for correlation length growth data: $\kappa = At^{\nu}$

	A		ν	
Sample	$A_{\|}$	$A_{\perp}$	$\nu_{\|}$	$\nu_{\perp}$
PS_1PI_1	0.86	0.68	0.07	0.06
PS_2PI_2	1.00	0.66	0.10	0.13
PS_4PI_4	0.59	0.49	0.14	0.13
$PS_{16}PI_{16}$	0.44	0.37	0.10	0.13

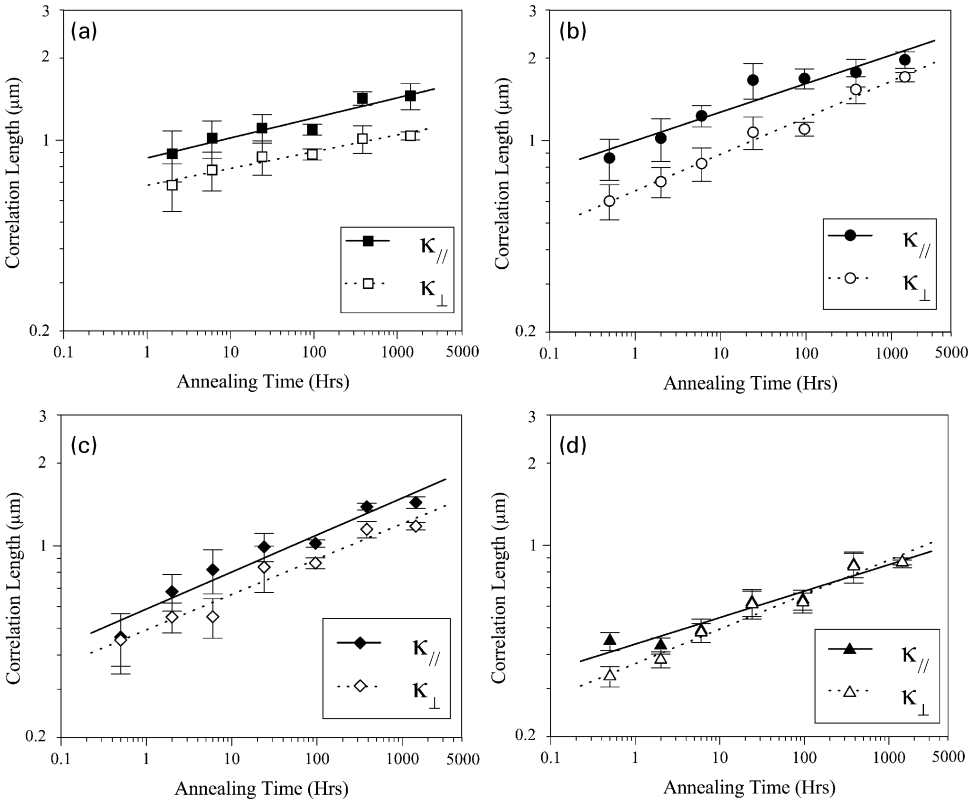

Fig. 3 The growth of correlation lengths in PS_nPI_n star block copolymers as a function of annealing time at 120 °C: (a) PS_1PI_1, (b) PS_2PI_2, (c) PS_4PI_4, and (d) $PS_{16}PI_{16}$. The lines in each plot are the least-squares, power law fits to the corresponding correlation length.

would eventually surpass that of the diblock. Grain growth experiments beyond the two-month maximum used in this study become difficult due to the limits of thermal and oxidative stability of the materials.

This data suggests a fundamental difference in the mechanisms of grain growth in the diblock verses all the A_nB_n stars for $n = 2$, 4, and 16. Dynamics in the case of the stars occurs by a faster type of mechanism than that of the diblocks. The increasing molecular weight as n increases from 2 to 16 in the A_nB_n series results in slower versions of the same mechanism. We hypothesize that the

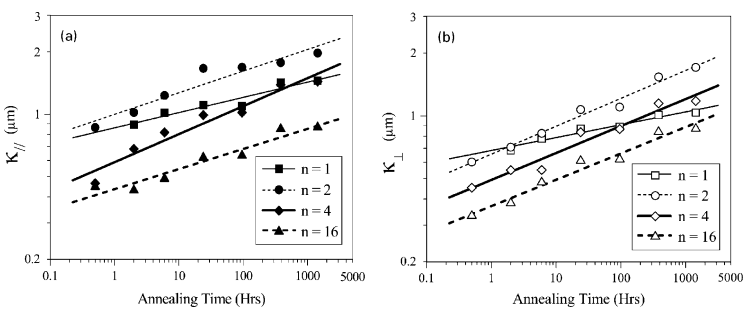

Fig. 4 The effect of arm number, n, on the growth of correlation lengths in PS_nPI_n star block copolymers as a function of annealing time at 120 °C: (a) $\kappa_{\|}$ values, (b) $\kappa_{\perp}$ values. The lines in each plot are the least-squares, power law fits to the corresponding correlation length.

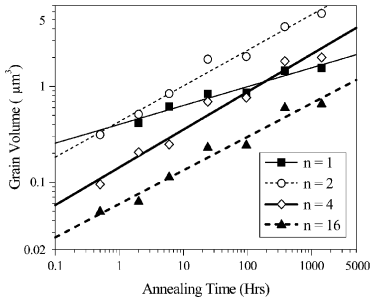

Fig. 5 The growth of grain volumes in PS_nPI_n star block copolymers as a function of annealing time at 120 °C: The lines in the plot are the least-squares, power law fits to the corresponding grain volume data.

Table 4 Power law fitting parameters for grain volume growth data: $V = A_v t^{\beta}$

Sample	A_v	β
PS_1PI_1	0.40	0.20 ± 0.02
PS_2PI_2	0.43	0.37 ± 0.02
PS_4PI_4	0.14	0.39 ± 0.03
$PS_{16}PI_{16}$	0.06	0.35 ± 0.03

difference between the diblock and the various A_nB_n stars is related to molecular entanglements. The molecular weight of the diblock suggests that it is slightly entangled. However, the previous work by Zhu, Gido and co-workers[35] shows that in the microphase separated state that the A_nB_n stars for $n = 2$, 4, and 16 are between 5 and 12% more stretched normal to the interface than the corresponding diblocks, due to the effect of arm crowding near the 2n functional junction point. This additional chain stretching normal to the interface may reduce entanglements with laterally neighboring chains thereby greatly increasing the rate at which the A_nB_n stars can diffuse within the lamellar layers relative to the corresponding rate for the entangled diblocks.[52–58] The diblock grains start out ($t = 0$) larger than the grains in the A_4B_4 and $A_{16}B_{16}$ samples due to the solvent casting process used to prepare the initial samples. The grains of the initial states for all samples are formed during solvent casting, where the diluting effect of the solvent will reduce the entanglements of the diblock during much if not all of the initial grain growth process. Once the solvent is fully removed, however, all the A_nB_n stars have faster growing grains, and even the A_4B_4 and $A_{16}B_{16}$ grain sizes should pass that of the diblock given enough time.

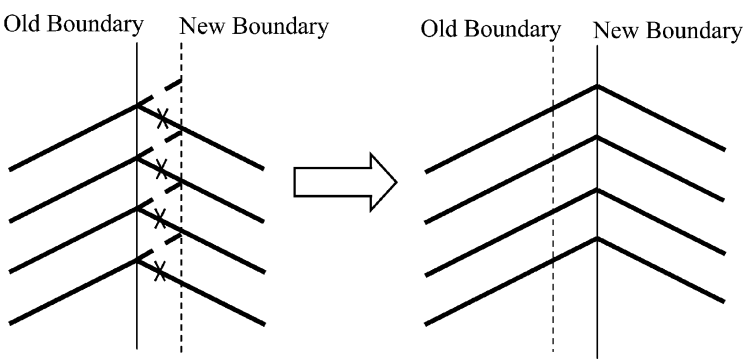

Fig. 6 Schematic of motion of a chevron tilt grain boundary. If the lamellar orientation on either side of the boundary is to be preserved, then the motion must involve the breaking and reforming of interfaces as indicated by ×'s and dashed lines in the diagram.

Conclusions

The scaling relationships we find for grain size growth as a function of time bears no simply discernible relationship to the kinetics of either entangled or unentangled block copolymer diffusion within, or normal to, lamellar layers as studied by Lodge and co-workers.[54–58] This is not necessarily surprising since the relationship between grain growth in three dimensions and diffusion of chains along two dimensional interfaces is likely complex and has not been elucidated. Simple geometric arguments, illustrated in Fig. 6, suggest that tilt grain boundaries (both symmetric and asymmetric) cannot move by molecular motions along the interface alone. Some interfacial breaking and reforming (*i.e.* diffusion of chains normal to the lamellar layers) is necessary to move this type of grain boundary. It may be possible for twist grain boundaries with Scherk saddle surface interfaces[59,60] to move through the sample *via* a mechanism in which the interfaces remain intact, *i.e.* only diffusion along existing interfaces is required. If this is true, then twist grain boundaries may move faster than tilt grain boundaries. However, any polygrain sample contains both twist and tilt boundaries as well as compound grain boundaries containing both twist and tilt character. Thus the situation is very complex.

Acknowledgements

S.P.Gido acknowledges funding from the U.S. Army Research Laboratory. The authors acknowledge Prof. Nitash P. Balsara for helpful discussion on ordering kinetics. The authors also acknowledge the use of central facility and the W. M. Keck Electron Microscopy in the Material Research Science and Engineering Center (MRSEC) at the University of Massachusetts–Amherst.

References

1 L. Leibler, *Macromolecules*, 1980, **13**, 1602.
2 K. Kawasaki and A. Onuki, *Phys. Rev. A*, 1990, **42**, 3664.
3 J. Csernica, R. F. Baddour and R. E. Cohen, *Macromolecules*, 1989, **22**, 1493.
4 D. H. Rein, J. Csernica, R. F. Baddour and R. E. Cohen, *Macromolecules*, 1990, **23**, 4456.
5 J. Csernica, R. F. Baddour and R. E. Cohen, *Macromolecules*, 1990, **23**, 1429.
6 M. Park, C. Harrison, P. M. Chaikin, R. A. Register and D. H. Adamson, *Science*, 1997, **276**, 1401.
7 R. R. Li, P. D. Dapkus, M. E. Thompson, W. G. Jeong, C. Harrison, P. M. Chaikin, R. A. Register and D. H. Adamson, *Appl. Phys. Lett.*, 2000, **76**, 1689.
8 K. Amundson, E. Helfand, X. Quan and S. D. Smith, *Macromolecules*, 1993, **26**, 2698.
9 K. Amundson, E. Helfand, X. N. Quan, S. D. Hudson and S. D. Smith, *Macromolecules*, 1994, **27**, 6559.
10 B. Ashok, M. Muthukumar and T. P. Russell, *J. Chem. Phys.*, 2001, **115**, 1559.
11 T. Xu, C. J. Hawker and T. P. Russell, *Macromolecules*, 2003, **36**, 6178.
12 Y. Tsori, F. Tournilhac and L. Leibler, *Macromolecules*, 2003, **36**, 5873.
13 G. G. Pereira and D. R. M. Williams, *Macromolecules*, 1999, **32**, 8115.
14 E. Huang, T. P. Russell, C. Harrison, P. M. Chaikin, R. A. Register, C. J. Hawker and J. Mays, *Macromolecules*, 1998, **31**, 7641.
15 E. Huang, S. Pruzinsky, T. P. Russell, J. Mays and C. J. Hawker, *Macromolecules*, 1999, **32**, 5299.
16 P. Mansky, T. P. Russell, C. J. Hawker, M. Pitsikalis and J. Mays, *Macromolecules*, 1997, **30**, 6810.
17 N. P. Balsara and B. Hammouda, *Phys. Rev. Lett.*, 1994, **72**, 360.
18 B. J. Dair, A. Avgeropoulos, N. Hadjichristidis, M. Capel and E. L. Thomas, *Polymer*, 2000, **41**, 6231.
19 T. J. Hermel, L. F. Wu, S. F. Hahn, T. P. Lodge and F. S. Bates, *Macromolecules*, 2002, **35**, 4685.
20 J. Bodycomb, Y. Funaki, K. Kimishima and T. Hashimoto, *Macromolecules*, 1999, **32**, 2075.
21 C. R. Harkless, M. A. Singh, S. E. Nagler, G. B. Stephenson and J. L. Jordansweet, *Phys. Rev. Lett.*, 1990, **64**, 2285.
22 M. A. Singh, C. R. Harkless, S. E. Nagler, R. F. Shannon and S. S. Ghosh, *Phys. Rev. B*, 1993, **47**, 8425.
23 R. T. Myers, R. E. Cohen and A. Bellare, *Macromolecules*, 1999, **32**, 2706.
24 M. Y. Chang, F. M. Abuzaina, W. G. Kim, J. P. Gupton, B. A. Garetz, M. C. Newstein, N. P. Balsara, L. Yang, S. P. Gido, R. E. Cohen, Y. Boontongkong and A. Bellare, *Macromolecules*, 2002, **35**, 4437.
25 F. L. Beyer, S. P. Gido, C. Buschl, H. Iatrou, D. Uhrig, J. W. Mays, M. Y. Chang, B. A. Garetz, N. P. Balsara, N. B. Tan and N. Hadjichristidis, *Macromolecules*, 2000, **33**, 2039.
26 H. Wang, M. C. Newstein, M. Y. Chang, N. P. Balsara and B. A. Garetz, *Macromolecules*, 2000, **33**, 3719.
27 M. C. Newstein, B. A. Garetz, N. P. Balsara, M. Y. Chang and H. J. Dai, *Macromolecules*, 1998, **31**, 64.
28 W. G. Kim, B. A. Garetz, M. C. Newstein and N. P. Balsara, *J. Polym. Sci. Part B*, 2001, **39**, 2231.

29 C. Harrison, D. H. Adamson, Z. D. Cheng, J. M. Sebastian, S. Sethuraman, D. A. Huse, R. A. Register and P. M. Chaikin, *Science*, 2000, **290**, 1558.
30 H. J. Dai, N. P. Balsara, B. A. Garetz and M. C. Newstein, *Phys. Rev. Lett*., 1996, **77**, 3677.
31 W. G. Kim, M. Y. Chang, B. A. Garetz, M. C. Newstein, N. P. Balsara, J. H. Lee, H. Hahn and S. S. Patel, *J. Chem. Phys*., 2001, **114**, 10 196.
32 N. P. Balsara, B. A. Garetz, M. Y. Chang, H. J. Dal and M. C. Newstein, *Macromolecules*, 1998, **31**, 5309.
33 S. T. Milner, *Macromolecules*, 1994, **27**, 2333.
34 D. M. A. Buzza, I. W. Hamley, A. H. Fzea, M. Moniruzzaman, J. B. Allgaier, R. N. Young, P. D. Olmsted and T. C. B. McLeish, *Macromolecules*, 1999, **32**, 7483.
35 Y. Q. Zhu, S. P. Gido, M. Moshakou, H. Iatrou, N. Hadjichristidis, S. Park and T. Chang, *Macromolecules*, 2003, **36**, 5719.
36 V. Grayer, E. E. Dormidontova, G. Hadziioannou and C. Tsitsilianis, *Macromolecules*, 2000, **33**, 6330.
37 M. W. Matsen and J. M. Gardiner, *J. Chem. Phys*., 2000, **113**, 1673.
38 D. M. A. Buzza, A. H. Fzea, J. B. Allgaier, R. N. Young, R. J. Hawkins, I. W. Hamley, T. C. B. McLeish and T. P. Lodge, *Macromolecules*, 2000, **33**, 8399.
39 A. Jabbarzadeh, J. D. Atkinson and R. I. Tanner, *Macromolecules*, 2003, **36**, 5020.
40 K. Chrissopoulou, Y. Tselikas, S. H. Anastasiadis, G. Fytas, A. N. Semenov, G. Fleischer, N. Hadjichristidis and E. L. Thomas, *Macromolecules*, 1999, **32**, 5115.
41 K. Chrissopoulou, S. Harville, S. H. Anastasiadis, G. Fytas, J. W. Mays and N. Hadjichristidis, *J. Polym. Sci. Part B*, 1999, **37**, 3385.
42 J. Allgaier, R. N. Young, V. Efstratiadis and N. Hadjichristidis, *Macromolecules*, 1996, **29**, 1794.
43 H. Iatrou and N. Hadjichristidis, *Macromolecules*, 1993, **26**, 2479.
44 R. P. Quirk, T. Yoo and B. J. Lee, *J. Macromol. Sci., Pure Appl. Chem*., 1994, **31**, 911.
45 Y. Q. Zhu, R. Weidisch, S. P. Gido, G. Velis and N. Hadjichristidis, *Macromolecules*, 2002, **35**, 5903.
46 F. L. Beyer, S. P. Gido, D. Uhrig, J. W. Mays, N. B. Tan and S. F. Trevino, *Journal of Polymer Science Part B-Polymer Physics*, 1999, **37**, 3392.
47 F. L. Beyer, S. P. Gido, Y. Poulos, A. Avgeropoulos and N. Hadjichristidis, *Macromolecules*, 1997, **30**, 2373.
48 F. L. Beyer, S. P. Gido, G. Velis, N. Hadjichristidis and N. B. Tan, *Macromolecules*, 1999, **32**, 6604.
49 B. A. Garetz, N. P. Balsara, H. J. Dai, Z. Wang, M. C. Newstein and B. Majumdar, *Macromolecules*, 1996, **29**, 4675.
50 N. P. Balsara, C. M. Marques, B. A. Garetz, M. C. Newstein and S. P. Gido, *Phys. Rev. E*, 2002, **66**.
51 T. Hashimoto and N. Sakamoto, *Macromolecules*, 1995, **28**, 4779.
52 D. Ehlich, M. Takenaka, S. Okamoto and T. Hashimoto, *Macromolecules*, 1993, **26**, 189.
53 D. Ehlich, M. Takenaka and T. Hashimoto, *Macromolecules*, 1993, **26**, 492.
54 M. C. Dalvi and T. P. Lodge, *Macromolecules*, 1993, **26**, 859.
55 M. C. Dalvi, C. E. Eastman and T. P. Lodge, *Phys. Rev. Lett*., 1993, **71**, 2591.
56 T. P. Lodge and M. C. Dalvi, *Phys. Rev. Lett*., 1995, **75**, 657.
57 T. P. Lodge, M. W. Hamersky, J. M. Milhaupt, R. M. Kannan, M. C. Dalvi and C. E. Eastman, *Macromol. Symp*., 1997, **121**, 219.
58 M. W. Hamersky, M. Tirrell and T. P. Lodge, *Langmuir*, 1998, **14**, 6974.
59 S. P. Gido, J. Gunther, E. L. Thomas and D. Hoffman, *Macromolecules*, 1993, **26**, 4506.
60 S. P. Gido and E. L. Thomas, *Macromolecules*, 1994, **27**, 849.